Porphyromonas gingivalis outer membrane vesicles alter neuronal architecture and Tau phosphorylation in the embryonic mouse brain

Adrienne Bradley[1 ¶], Lauren Mashburn-Warren[1 ¶], Lexie C. Blalock[1 ¶ #a], Francesca Scarpetti[1], Christian L. Lauber[1,2*]

[1] Institute for Genomic Medicine, Nationwide Children's Hospital, Columbus, Ohio, USA

[2] Department of Pediatrics, The Ohio State University College of Medicine, Columbus, Ohio, USA

[#a] Current Address: Microbiology/Allergen Control, Global Analytical & Food Safety, Abbott Nutrition, Columbus, Ohio, USA

*Corresponding Author

E-mail: Christian.Lauber@nationwidechildrens.org

¶ These authors contributed equally to this work.

Abstract

Porphyromonas gingivalis (Pg) is an oral bacterial pathogen that has been associated with systemic inflammation and adverse pregnancy outcomes such as low birth weight and pre-term birth. Pg drives these sequalae through virulence factors decorating the outer membrane that are present on non-replicative outer membrane vesicles (OMV) that are suspected to be transmitted systemically. Given that Pg abundance can increase during pregnancy, it is not well known whether Pg-OMV can have deleterious effects on the brain of the developing fetus. We tested this possibility by treating pregnant C57/Bl6 mice with PBS (control) and OMV from ATCC 33277 by tail vein injection every other day from gestational age 3 to 17. At gestational age 18.5, we measured dam and pup weights and collected pup brains to quantify changes in inflammation, cortical neuron density, and Tau phosphorylated at Thr231. Dam and pup weights were not altered by Pg-OMV exposure, but pup brain weight was significantly decreased in the Pg-OMV treatment group. We found a significant increase of Iba-1, indicative of microglia activation, although the overall levels of IL-1β, IL-6, TNFα, IL-4, IL-10, and TGFβ mRNA transcripts were not different between the treatment groups. Differences in IL-1β, IL-6, and TNFα concentrations by ELISA showed IL-6 was significantly lower in Pg-OMV brains. Cortical neuron density was modified by treatment with Pg-OMV as immunofluorescence showed significant decreases in Cux1 and SatB2. Overall Thr231 was increased in pups exposed to Pg-OMV with the appearance of a secondary band of 60 kD. Together these results demonstrate that Pg-OMV can significantly modify the embryonic brain and suggests that Pg may impact offspring development via multiple mechanisms.

Introduction

Pregnancy induces significant changes in mothers including shifts in the abundance of oral bacteria (1-4). Increased blood flow and pregnancy related hormones allows for the growth of pathogens like *Porphyromonas gingivalis* (Pg) an organism associated with oral infections that are increasingly linked to adverse pregnancy and neurodevelopmental outcomes (5-7). Increased Pg presence is estimated to be prevalent in 40% of pregnancies in the US and 2-11% worldwide (8, 9). This presence of bacteria sometimes resulting in periodontitis, a significant dental infection, can drive systemic inflammation (10-12). Preterm birth, preeclampsia, and low birth weight are well-characterized effects of maternal Pg infections and Pg DNA has been detected in the placenta and amnionic fluid. Pg driven outcomes affecting children have focused on pregnancy outcomes (13-18) and only recently has Pg received attention as a modulator of fetal development and remains an understudied host-pathogen interaction (19, 20).

P. gingivalis has been extensively studied to determine its role in modifying pregnancy. Rodent models of Pg infection demonstrate that exposure to Pg can result in systemic inflammation, low birth weight and pre-term delivery (21-25). Pg mediates these and other effects thorough a number of virulence factors that modify host responses including lipopolysaccharide (LPS) and proteases known as gingipains (26-32). Both are also present on the surface of OMV that are now suspected to be transmitted systemically in the blood stream (20, 32, 33). LPS and the gingipains interact with the immune system but are unique compared to other gram-negative bacteria. For instance, Pg LPS is less immunogenic than *Escherichia coli* LPS but also causes inflammation and the production

72 of pro-inflammatory cytokines (34, 35). The gingipains are unique to Pg and they modify
73 cytokine expression that allows Pg to evade the host immune response and establish
74 periodontal infections that drive systemic inflammation (36-39). Pg infection also modifies
75 the placenta to cause spiral artery remodeling that can result in a hypoxic state linked to
76 preeclampsia and fetal growth restriction (40). However, whether Pg-OMV may induce
77 fetal growth restriction—a common outcome in animal models and humans with Pg
78 infections of clinical significance—is not yet known.
79
80 *P. gingivalis* is associated with maternal inflammation and adverse pregnancy outcomes
81 that increase the risk of modified developmental trajectories of offspring (17, 41). Live Pg
82 is well demonstrated to increase inflammation in animal models and exposure to Pg-OMV
83 recapitulates these observations as the vesicles harbor the same virulence factors. Ishida
84 et al. reported increased Iba-1 indicative of microglia activation and modified
85 neuroarchitecture in E 20 pup brains from dams with an established Pg infection prior to
86 pregnancy (19). These alterations were accompanied by declines in cognitive ability, and
87 it was suggested the combined effects on the embryonic brain resulted in
88 neuroinflammation that drove these changes. Similarly, Gong et al. described a
89 neuroinflammatory phenotype in adult mice where exposure to Pg-OMV for 3 months
90 increased IL-1β and NLRP3 expression concurrent with modification of the
91 neuroarchitecture and behavior (33). Together these studies suggest that long-term
92 exposure to Pg and Pg-OMV can result in immune phenotypes indicative of a pro-
93 inflammatory response that would be expected from activated microglia in the M1
94 activation state (42, 43). However, the maternal immune system functions differently than

95 the non-pregnant state and changes in inflammation and neuroarchitecture related to
96 pathogen exposure *in utero* after pregnancy is establish may also differ. This knowledge
97 gap limits our efforts to refine predictions of the potential impact of pathogen-driven
98 inflammation on the developmental trajectory of offspring.
99
100 Tau is an essential protein with multiple roles in maintaining neuron homeostasis (44-46).
101 Proper function is dependent on phosphorylation that can occur at multiple sites and can
102 be modified by inflammation and exposure to pathogens such as Pg (47-49).
103 Phosphorylated Tau (p-Tau) has less affinity for tubulins and self-aggregates into β-
104 amyloid plaques that are a hallmark of neuroinflammatory diseases such as Alzheimer's
105 and Parkinson's diseases in older adults (50). The resulting tau tangles can trigger an
106 immune response that is sustained through microglial NFκβ signaling and thus are
107 considered pathogenic forms of the protein (51, 52). In a mouse model, Gong et al.
108 showed that Pg-OMV alter the tau profile and could result in β-amyloid plaques
109 accompanied by increased inflammation (33). However, relatively less is known about the
110 role of p-Tau in the developing brain and whether exposure to pathogens during
111 pregnancy alters this profile. A survey of fetal and adult Tau phosphorylation in humans
112 demonstrated significant overlap in p-Tau where some of the pathogenic forms of Tau in
113 adults with Alzheimer's disease were also prevalent in the fetal brain suggesting p-Tau in
114 children does not have a pathogenic effect as observed in adults (53). Interestingly, Tau
115 is hyperphosphorylated in the embryonic rodent brain but knock-down of Tau during
116 gestation in mice can reduce neuronal migration to all cortical layers indicating that p-Tau
117 is an important part of normal brain development in mice (47, 49, 54). Whether or not Pg-

118 OMV may modulate Tau phosphorylation in developing brains *in utero* is an open
119 question. Addressing this knowledge gap may provide valuable insight into the
120 mechanisms by which Pg is able to modify developmental trajectories of children.
121
122 Herein, we describe a study to determine the effect of Pg-OMV on the developing mouse
123 brain to understand this host-pathogen interaction that frequently occurs in the human
124 population. To simulate a maternal infection with Pg, pregnant C57/Bl6 mice were
125 exposed to a consistent dose of Pg-OMV via tail vein injection. At gestational age (GA)
126 18.5, inflammatory responses, concentration of Tau Thr231 (Thr231) and neuron density
127 in the cortices of embryonic pup brains were assessed to augment the understanding of
128 Pg-modulated brain development that may be relevant to pathogen exposure during
129 pregnancy.
130

131 Results

132 Pup Body and Brain Weights

133 Previous studies in mice have demonstrated that dams with Pg infection or those
134 consistently dosed with Pg bacteria during pregnancy can result in low birth weight of
135 pups. We recorded weight of the dams, pups, and pup brains at GA 18.5 (Fig 1A) to
136 determine whether exposure to Pg-OMV would have the same effect. Dam and pup
137 weights were not significantly different in PBS and Pg-OMV groups (Fig 1B and 1C) but
138 there was a significant decrease in the pup brain weight after 14 days of Pg-OMV
139 treatment (Fig 1D, Mann-Whitney U $p = 0.023$,). We included an assessment of Hif1a as
140 Pg is known to cause hypoxia in mouse models that is related to fetal growth restriction.

141 Relative expression of HiF1a in the embryonic mouse brain was not significantly different
142 between the control and treated groups indicating the OMV did not induce a hypoxic state
143 *in utero* that could account for the decreased pup brain weights (Fig 1E).
144
145 **Fig 1. Experimental design and pup body and brain weights.**
146 (A) C57/Bl6 mice were mated for up to 3 days until the appearance of vaginal plugs. The
147 first observation of a plug was considered GA 0. Female mice were separated from the
148 males and treated with PBS or 50 ug Pg-OMV every other day from GA 3 to GA17. Dams
149 were sacrificed on GA 18.5 and pups delivered by C-Section for tissue collection. (B) and
150 (C) Weight of dams and pups were not significantly different from PBS controls. (D) Brain
151 weight decreased significantly with Pg exposure (Mann-Whitney U $p = 0.023$). (E)
152 Relative expression of Hif1a as indicator of hypoxia in the pup brain. Relative expression
153 calculated by the $2^{-(\Delta\Delta Ct)}$ method with GAPDH as the reference gene. Data are shown as
154 median with 95% CI.
155

156 Inflammation

157 Maternal inflammation can affect the developing embryo in mouse models, and we tested
158 whether exposure to Pg-OMV during pregnancy would result in an inflammatory response
159 concordant with increased presence of pathogens experienced during pregnancy. First,
160 we assessed the concentration of Iba-1 as a surrogate of microglia activation and
161 established this immune cell typically involved in pathogen defense was active in the
162 embryonic mouse brain. Western blotting of whole brain homogenates showed that Iba-
163 1 was significantly increased in Pg-OMV pup brains compared to PBS controls (Fig 2A

164 and 2B, Mann-Whitney U $p = 0.0003$). Next, we tested whether increased Iba-1 was
165 accompanied by increased concentration and expression of pro-inflammatory cytokines
166 IL-1β, IL-6 and TNFα indicative of M1 activation that produces a pro-inflammatory
167 response. ELISA quantification showed that PBS pups typically had higher levels of
168 cytokines but only IL-6 was significantly greater in the PBS brains compared to pups from
169 the Pg-OMV group (Fig 3D, Student's T-test $p = 0.002$). The levels of IL-1β and TNFα
170 showed similar trends but were not statistically different between the treatment groups
171 (Fig 3A, 3D, 3G, $p > 0.05$ in all cases). We extended this analysis to include effects that
172 may be apparent at the level of expression in the embryonic brain tissue. RT-qPCR
173 analysis of these cytokines showed no significant difference between the PBS and Pg-
174 OMV pups. Then, we tested the possibility that increased Iba-1 could result in an M2 or
175 anti-inflammatory immune response given that microglia can be in two broad functional
176 categories (42, 55). Analysis of IL-4, IL-10 and TGFβ typical of M2 activated microglia
177 were not significantly different between the treatment groups (Fig 3 C, 3F, 3I, $p > 0.05$ in
178 all cases). Lastly, given these results we tested whether the expression of NLRP3, MyD88
179 and NFκβ, that can be modified by exposure to Pg or it's OMV, were also modified in our
180 pups. RT-qPCR analysis of MyD88 and NLRP3 transcripts (Fig 4) had similar downward
181 trends with Pg-OMV treatment but were not significantly different compared to controls
182 (Fig 4A, and 4B, $p > 0.05$ in both cases). Interestingly, NFkβ transcripts that are typically
183 reported as being upregulated by Pg were significantly decreased in the Pg-OMV group
184 (Fig 4C, Student's T-test $p = 0.004$).
185
186 **Fig 2. Increased Iba-1 in mouse pups exposed to Pg-OMV during pregnancy.**

187 **(A)** Western blot of Iba-1 and β-actin in GA 18.5 pups from PBS and Pg-OMV exposed
188 dams. Full blot can be found in the Supporting information. **(B)** Comparison of band β-
189 actin normalized signal intensity of Iba-1 showed significant increase in Iba-1 in the Pg-
190 OMV group compared to controls (Mann-Whitney U p = 0.0003). Data are shown as
191 median with 95% CI.
192
193 **Fig 3. ELISA and RT-qPCR evaluation of cytokines in the embryonic mouse brain.**
194 **(A, D, G)**: ELISA of IL-1β, IL-6, and TNFα in pg ml^{-1}. Cytokines were extracted from frozen
195 whole brains and quantified. IL-1β was significantly greater in the PBS female pups
196 compared to the female pups from the Pg-OMV group (Fig 3A, Mann-Whitney U test p =
197 0.04). IL-6 was significantly greater in the PBS group and in the female pups compared
198 to the OMV treatment group (Fig 3D, Student's T-test p = 0.002 and 0.0095, respectively.)
199 **(B, E, H)**: RT-qPCR of proinflammatory cytokines IL-1β, IL-6, and TNFα. **(C, F, I)**: RT-
200 qPCR of anti-inflammatory cytokines IL-4, IL-10, and TGFβ. Total RNA was extracted
201 from frozen whole brains and reverse transcribed to cDNA. Relative expression
202 calculated by the $2^{-(\Delta\Delta Ct)}$ method with GAPDH as the reference gene. Group differences
203 for the ELISAs on the males was not determined due to low sample size (n = 2). Only
204 significant differences are shown. Data are presented with the median and 95% CI.
205 Symbols: Circles = PBS, triangles = Pg; orange = females; blue = males.
206
207 **Fig 4. RT-qPCR evaluation of MYD88, NLRP3, and NFκβ in GA 18.5 pup brains.**
208 **(A)** MYD88 and **(B)** NLRP3 were not significantly different in pup brains from the control
209 or treatment group. **(C)** NFkβ was significantly reduced in the pup brains (Student's T-test

210 p = 0.004). Total RNA was extracted from frozen whole brains and reverse transcribed to
211 cDNA. Relative expression calculated by the $2^{-(\Delta\Delta Ct)}$ method with GAPDH as the
212 reference gene. Means across fore, mid, and hind brain sections are shown for each
213 sample. Data are presented with the median value and 95% CI.
214
215 We were interested in identifying potential modifications in cytokine concentration and
216 expression that may differ between female and male offspring as maternal inflammation
217 may have sex specific effects. When parsed by sex, we observed that IL-6 and IL-1β
218 concentrations were significantly lower in female pups from the Pg-OMV group compared
219 to the female controls (Fig 3A, Mann-Whitney U test p = 0.04 and 3D, Student's T-test p
220 = 0.0095) and though TNFα was lower in Pg-female pups, it was not statistically different
221 in our analysis (Fig 3A, 3D. 3G). The effect of Pg-OMV on transcription was highly variable
222 for IL-1β, TNFα, IL-4, IL-10 and TGFβ but generally trended upwards (Fig 3B-3I) for the
223 female pups. Trends in the males were similar but were not significant and likely result
224 from low sample sizes (Fig 3), though we could not assess difference in cytokine
225 concentrations as the Pg male group had only 2 observations (Fig 3A, 3D, 3G).
226

227 **Neuroarchitecture**

228 Without a strong inflammatory phenotype, we tested the possibility that Pg-OMV
229 treatment could nonetheless result in differences in the neuroarchitecture of the
230 developing mouse brain. We examined the distribution of neuronal proteins Cux1, SatB2,
231 and Ctip2 that are differentially expressed across the layers of the cortex in sagittal
232 sections of-embryonic mouse brains. The distribution and density of these proteins were

233 modified by exposure to Pg-OMV compared to pups from the PBS group (Fig 5A and 5B).
234 We saw significant decreases in Cux1 (Student's T-test p = 0.03) and SatB2 (Students
235 T-test p = 0.0001) signal intensity but not Ctip2 (Student's T-test p = 0.064) although it
236 also followed a similar downward trend in the Pg-OMV pup brains (Fig 5B). These findings
237 suggests that cortical layering was drastically altered in Pg exposed animals.
238
239 **Fig 5. Modified intensity and location of cortical layer marker proteins following Pg-**
240 **OMV exposure *in utero*. (A)** Representative immunofluorescent images from sagittal
241 sections of PFA fixed brains at GA 18.5 pup brains showing location of cortical layer
242 markers Cux1, SatB2, and Ctip2. Approximate position of cortical layers 1-6 with the
243 intraventricular zone (IZ) are shown in the PBS-DAPI image. **(B)** Quantification and
244 comparison of cortical layer proteins stained with the marker antibodies. Intensities were
245 averaged across three serial section per sample for statistical analysis. Cux1 (Student's
246 T-test p = 0.03) and SatB2 (students T-test p = 0.0001) were significantly reduced in the
247 Pg-OMV group. Data are presented with the median and 95% CI.
248
249 ## Tau Thr231
250 We evaluated whether Tau phosphorylated at Thr231 in GA 18.5 mouse brains was
251 affected by exposure to Pg-OMV during gestation as this is one form of p-Tau implicated
252 in neuroinflammatory diseases. Western blotting of proteins from whole brain
253 homogenates showed Thr231 was present in PBS and Pg-OMV mouse brains at
254 approximately 50 kD indicating that at this amnio acid, Tau was in a phosphorylated state
255 concordant with other observations of Tau in the developing mouse brain (Fig 6A). We
256 observed that an additional band at 60kD became more prominent in the Pg-OMV brains

257 compared to controls (Fig 6A). Quantification of these bands showed that both the 50kD
258 and 60kD bands were significantly greater in the brains from Pg-OMV exposed mice
259 compared to the PBS control group (Fig 6B, 50 kD Student's T-test p = 0.003, 60kD
260 Student's T-test p = 0.0006). The increased abundance of both (e.g. 50kD signal + 60kD
261 signal = total Thr231) lead to significant overall increase of Thr231 in the Pg-OMV group
262 (Fig 6B, total Thr231, Student's T-test p = 0.001) indicating Pg-OMV may alter the total
263 concentration and diversity of Thr231 isoforms during development in our mice.
264
265 **Fig 6. Thr231 is elevated in the embryonic mouse brain after exposure to Pg-OMV.**
266 **(A)** Images of Thr231 western blots. 20 ug of total protein extracted from whole, frozen
267 GA 18.5 pup brains were analyzed. A band of approximately 60 kD became more
268 prominent in the brains of all pups exposed to Pg-OMV during pregnancy.
269 **(B)** Densitometry analysis of Thr231 abundance by western blot normalized to vinculin.
270 Total Thr231 was estimated by summing the vinculin normalized intensity of the 50 kD +
271 60 kD bands. Total Thr231 (Student's T-test p = 0.001), 50kD (Student's T-test p = 0.003)
272 and 60kD Thr231 quantities (Student's T-test p = 0.0006) were significantly greater in the
273 Pg-OMV brains. Data are presented with the median and 95% CI.
274

275 Discussion

276 Animal models of Pg infection demonstrate modified pregnancy outcomes and can alter
277 birth weight of offspring. Our experimental design did not recapitulate these observations
278 as pup weights in the Pg-OMV group were not statistically different from PBS controls.
279 Moreover, dam weights were also unchanged indicating that food and water intake were

280 likely not different between the control and treatment groups. The mechanism behind
281 reduced brain weight is not clear from our observations, although pup weight followed a
282 similar downward trend suggesting that the effect of Pg-OMV was systemic for the
283 developing embryos. It could be possible that exposure to pathogens after initiation of
284 pregnancy is different from a state where the pathogen is already present and interacting
285 with host defense mechanisms. Likewise, the dosage of Pg-OMV we used may have not
286 been sufficient to recapitulate the full effect of Pg on pregnancy outcomes, where more
287 robust responses of the host and fetus may be required to lower birth weights. This would
288 coincide with unchanged expression of Hif1a. Nevertheless, treatment with a low dosage
289 of Pg-OMV during pregnancy impacted the development of the embryonic brain that could
290 have implications after birth.
291
292 *P. gingivalis* and Pg-OMV induced neuroinflammation is suspected to be involved in
293 cognitive decline in aging cohorts and have a significant impact on development *in utero*.
294 Our hypothesis that Pg-OMV would produce a pro-inflammatory response in the
295 embryonic mouse brain was not observed. Cytokine concentrations and levels of mRNA
296 transcripts in the pup brains tended to be lower in the Pg-OMV group. The lack of
297 concordance with previous work was somewhat unexpected as most reports demonstrate
298 systemic inflammation upon exposure to Pg or its OMV. Significant increases of Iba-1 in
299 Pg-OMV exposed brains indicates sensing of bacterial-derived components, such as
300 LPS, that can stimulate immune response, though this was not accompanied by a
301 significant increase in cytokine production in our mice. Moreover, Pg has atypical LPS
302 compared to organisms like *E. coli* LPS, that can bind to TLR-4, but can be recognized

303 by alternative sensing pathways (Refs). We addressed this possibility by quantifying the
304 expression of MYD88 and NLRP3 inflammasome mRNAs that are known to increase
305 upon exposure to Pg or Pg-OMV. Our analysis found that concentrations of both were
306 unaffected by OMV treatment in GA 18.5 pup brains and we posit several factors may be
307 influencing our data. First, our results could originate from the delivery of Pg-OMV via tail
308 vein injection which bypass sensing mechanisms such as dendritic cells of the
309 gastrointestinal tract that would detect Pg and LPS being translocated from the oral cavity
310 in saliva. Second, it is equally possible that Pg-OMV induced inflammation reported
311 elsewhere may be an outcome in adult mice with long-term exposure to Pg or Pg-OMV
312 but may not necessarily be an outcome for exposure after pregnancy has been
313 established given the maternal immune system functions differently compared to the pre-
314 pregnancy state. Thus, our observations may not be comparable to reports that use Pg
315 infection or treatment with Pg or Pg-OMV at high doses over several weeks prior to
316 inducing pregnancy. Importantly, the dosing scheme described here suggests there is a
317 potential use of Pg-OMV as a proxy for bacteria to study effects on fetal tissues
318 independent of systemic inflammation driven by common oral pathogens that become
319 more prevalent during pregnancy. More work is needed to elucidate how the timing and
320 dosage of pathogen exposure relative to the start of pregnancy modulates immune
321 responses during gestation that could be associated with long-term consequences for
322 offspring in human populations.
323
324 Several reports have quantified the impact of Pg and Pg-OMV on neurons as that cell
325 type is affected by inflammation and is important in brain development. Our data indicate

326 that Pg-OMV have a significant impact on neurons as their prevalence was modified in
327 the cortical layers of the embryonic brain. Cux1, SatB2, and Ctip2 signals were lower
328 overall and showed modified distribution in the Pg-OMV exposed brains compared to
329 controls. The down regulation of SatB2 and Cux1 are particularly interesting as abnormal
330 expression of both are associated with altered behavior in mice and are suspected to be
331 a contributor to autism spectrum disorder-like symptoms in humans. Likewise,
332 deficiencies in Cux1 expression have been linked to neurodevelopmental delays, while
333 down regulation of Ctip2 is known to affect axonal growth and is involved in spiny neuron
334 differentiation (refs). The neuroarchitectural changes observed herein are aligned with
335 previous studies, yet novel because these cortical layer aberrations were not
336 accompanied by any indication of systemic inflammation. Collectively, these data suggest
337 that Pg, or perhaps Pg-OMV specially, affect the developing brain through a different
338 mechanism. Parsing out the effects of Pg-OMV on cell proliferation and migration appears
339 to be critical in deciphering how Pg mediates effects on the developing brain and should
340 be addressed in future studies to better understand this important host-pathogen
341 interaction.
342
343 The importance of Tau in the developing brain has not been fully described but our
344 observations indicate exposure to Pg-OMV can alter the amount of Thr231 in mouse
345 embryos. Tauopathies have multiple effects on the central nervous system including
346 sustained inflammation through NFκβ signaling microglia that detects the pathogenic form
347 of Tau in adult animal models. Our data would appear to support the notion that Thr231
348 in the embryonic mouse brain is not pathogenic as an innate immune response,

349 concordant with an inflammation-based hypothesis of neurodegenerative phenotypes,
350 was not observed. Accordingly, we did not observe an increase in NFκβ that can
351 encourage transcription of cytokines. We did not perform a comprehensive assessment
352 of Tau phosphorylation sites, nor did we specifically address potential interactions
353 between p-Tau and microglia. Nonetheless, the alteration of Thr231 abundance aids in
354 explaining how changes in neuron migration and axon growth may result from exposure
355 to Pg *in utero*; our observed changes in cortical layer markers could be the result of
356 altered microtubule binding driven by altered p-Tau. Thus, much work remains to be done
357 in elucidating the role of Pg and it OMV on human neurodevelopment and cognitive
358 trajectories from the early to elderly phases of life.
359

360 Methods

361 OMV Isolation

362 *Porphyromonas gingivalis* strain ATCC 33277 was grown in anaerobic conditions (85%
363 N_2, 10% CO_2, 5% H_2) using Tryptic Soy Broth (Difco cat# 211768) medium
364 supplemented with 5.0 mg ml-1 hemin (Thermo Fisher, cat# AAA1116503), 1.0 mg ml^{-1}
365 menadione (MP Biomedicals, cat # 102259), and 0.5 g L^{-1} L-cysteine-HC (MP
366 Biomedicals, cat # 101446). A cleared supernatant was produced by pelleting cells at
367 8000 rpm for 15 minutes followed by filtration of the supernatant through a 0.45 um
368 membrane filter under low vacuum pressure. Using Sorvall 11.5mL ultracentrifuge tubes
369 and ultracrimp tube plugs, filtered supernatant was ultacentrifuged at 65,000 rpm for 1
370 hour at 4°C using a Sorvall WX Ultra 80 centrifuge. Immediately after centrifugation,
371 supernatant was discarded and the pellet containing the OMV was resuspended in

372 500uL of PBS (56). The total protein of the OMV were quantified using the Pierce BCA
373 assay with BSA as a standard and stored at -20°C for future use.
374

375 Animal Breeding, Dosing and Tissue Collection

376 2-3 month old C57/Bl6 mice (male and female) were purchased from Jackson Labs
377 (Maine, USA). All animals were housed in the animal research core under 12 h light/dark
378 cycles. Mice were bred and dams were checked for plugs 2x/day. Once a plug was visible,
379 the dam was removed and was marked as gestational day 0 (GA 0). Starting at E3, 50
380 µg Pg OMV were administered via tail vein injection every other day until GA 18.5. An
381 equal volume of sterile PBS was used for the control group. Pregnant dams were
382 anesthetized using isoflurane and pups were removed via C-sections. C Pups were
383 decapitated and whole brain and placenta were collected from each pup. Half of the pup
384 brains were randomly chosen and fixed using 4% paraformaldehyde followed by 30%
385 sucrose prior to being mounted in O.C.T. and frozen for Immunohistochemical and
386 Immunofluorescent analysis. The remaining brains were snap frozen in a liquid N_2 at time
387 of collection and used for protein, RNA, and DNA extraction. Fixed tissues were stored at
388 4°C and frozen tissues were stored at -80°C. All experimental procedures were approved
389 by the IACUC under protocol AR21-00010.
390

391 Protein Extraction, Western Blotting and ELISA

392 Protein from snap-frozen whole brains were extracted using RIPA Buffer (cell signaling)
393 with protease inhibitor cocktail (ThermoFisher). Concentration was determined prior to

394 loading using the Pierce BCA Assay Kit (ThermoFisher) with subsequent colorimetric
395 detection using BioTek Synergy H1 microplate reader. Samples were denatured in
396 Laemmli buffer at 95°C for 5 min. 50 µg total protein from each sample was loaded onto
397 10% Mini-PROTEAN® TGX™ Precast Protein Gels (Bio-Rad) and separated for 1 h at
398 150 V. Proteins were transferred onto nitrocellulose or PVDF membranes using Turbo
399 transfer (Bio-Rad) for 7 min at 2.5 A. Membranes were incubated in Everyblot blocking
400 buffer (Bio-Rad) for 1 h at RT. For Iba-1 probe, membranes were cut at 37 kDa marker
401 and lower half was incubated with Iba1, top half was incubated with b-actin. For p-Tau,
402 membranes were cut between 75 and 100 kDa marker. Top half was incubated with
403 vinculin, bottom half was incubated with phospho-Tau (Thr231) from Cell Signaling (cat
404 # 71429). All primary antibody incubations were overnight at 4°C. Membranes were
405 washed in 1X Tris-buffered saline with 0.1% Tween-20 (TBST) prior to a secondary
406 incubation with either goat anti-mouse HRP or goat anti-rabbit HRP at a dilution of 1:3000
407 for 1 h at RT. Membranes were washed a second time with 1X TBST prior to a 5 min
408 incubation in ECL reagent (superSignal west pico plus ECL substrate kit). Blots were
409 imaged on a Bio-Rad Chemidoc. Densitometric analysis was performed in ImageLab
410 Software (Bio-Rad). Target signals were normalized to a control protein on each blot of
411 either Vinculin or β-actin. Aliquots of the RIPA extracted proteins (from above) were used
412 to quantify the cytokines by ELISA for IL-1β (Invitrogen IL-1 beta Mouse ELISA kit, cat #
413 BMS6002), IL-6 (Invitrogen IL-6 Mouse ELISA kit, cat # BMS603-2) and TNFα (Invitrogen
414 TNF alpha Mouse ELISA kit, cat # BMS607-3), from whole brains according to
415 manufacturer's protocol. All samples were run in duplicate. The average from both wells

416 was used for quantification. A full list of reagents and western blots can be found in
417 Supporting information S1 and S2.
418

419 Nucleic Acid Extraction, PCR, and RT-qPCR

420 DNA and RNA was extracted for sexing embryonic mice and RT-qPCR analysis of
421 cytokine mRNAs present in the pup brainst. Nucleic acids were extracted from frozen
422 whole brains using the Omega Bio-tek E.Z.N.A. kit according to manufacturer's protocol
423 (cat# R6731-01). RNA and DNA concentrations were determined using Qubit
424 Fluorometer (Applied Biosystems) prior to subsequent analysis. For sexing of pups we
425 added 1μL DNA to a reaction with the Q5 Master Mix (NEB, cat#) and primer sets for
426 amplification of the IL3 (For 5'- GGG ACT CCA AGC TTC AAT CA-3', Rev 5'- TGG AGG
427 AAG AAA AGC AA-3') and Sry (For 5'-TGG GAC TGG TGA CAA TTG TC, Rev 5'-GAG
428 TAC AGG TGT GCA GCT CT-3') genes (57). PCR conditions were 95°C for 4.5 min
429 followed by 33 cycles of 95°C for 35 s, 50°C for 1 min and 72°C for 1 min. PCR products
430 were terminated with a final extension at 72°C for 5 min. Bands positive for both are
431 labeled as male while samples only expressing IL3 are labeled as female.
432

433 cDNAs for RT-qPCR were made by adding 1000 ng RNA to a reaction using the High
434 Capacity cDNA Reverse Transcription Kit (Applied Biosystems, cat# 4368814). 1μL of
435 cDNA was added per reaction with gene specific primer pair sets for GAPDH, IL-1β, IL-
436 6, TNFα, IL-4, IL-10, and TGFβ (Integrated DNA Technologies, PrimeTime qPCR Primer
437 Assay). All samples were run in triplicate on a QuantStudio6 Pro (Applied Biosystems)
438 using the PowerUp SYBR Green Master Mix (ThermoFisher, cat # A25741). Cycling

439 conditions are as follows: 95°C for 15s followed by 60°C for 1 min for 40 cycles. Gene
440 expression was measured using the QuantStudio6 Pro detection system and normalized
441 to GAPDH. Ct values were averaged from each triplicate and used to calculate the relative
442 expression by the $2^{-(\Delta\Delta Ct)}$ method with GAPDH as the reference gene.
443

444 Immunofluorescent Staining

445 Fixed brains were embedded in OCT medium and 25 µm sagittal sections were collected
446 by a cryostat. Sections were washed with PBS, blocked in PBS containing 0.1% tritonX-
447 100, and 10% donkey serum and probed with and primary antibodies to Cux1 (Protein
448 Tech 11733-1-AP; diluted 1:300), SatB2 (Abcam ab92446; diluted 1:100), and Ctip2
449 (Abcam ab-18465; diluted 1:500). Sections were then washed with PBS and incubated
450 with Alexa Fluor® secondary antibodies (Thermo Fisher Scientific) and DAPI followed by
451 mounting with Prolong Diamond Antifade (Thermo Fisher Scientific). Images were
452 acquired with an ImageXpress Micro Confocal High Content Imaging System (IXMC;
453 Molecular Devices) and analyzed using MetaXpress software (Molecular Devices).
454

455 Data Analysis

456 We used the analysis routines in GraphPad PRISM v. 10.0 to perform statistical analysis
457 and plotting of data points. Outlier data points were identified by the ROUT method with
458 Q = 1% and removed from analysis. Data were tested for normality with the Kolmogorov-
459 Smirnov test. Group differences for data with normal distributions were tested with the
460 two-tailed, unpaired Student's-test, otherwise statistical differences were determined with

461 the Mann Whitney-U test. Data are presented with the median and 95% Confidence
462 Interval (CI).

463 # Acknowledgments

464 We thank Dr. Rolf Stottmann and Dr. Tracy Bedrosian in the Institute for Genomic Medicine for
465 their guidance on collecting and analyzing the cortical neurons of the embryonic mouse brains.
466 We also thank Dr. Juhi Bagaitkar in the Center for Microbial Pathogenesis at Nationwide
467 Children's Hospital or her discussions on the immunological implications of *P. gingivalis* infection.

468

469 # References

470

471 1. Carrillo-de-Albornoz A, Figuero E, Herrera D, Bascones-Martínez A. Gingival
472 changes during pregnancy: II. Influence of hormonal variations on the subgingival
473 biofilm. Journal of Clinical Periodontology. 2010;37(3):230-40.
474 2. Fujiwara N, Tsuruda K, Iwamoto Y, Kato F, Odaki T, Yamane N, et al. Significant
475 increase of oral bacteria in the early pregnancy period in Japanese women. Journal of
476 Investigative and Clinical Dentistry. 2017;8(1):e12189.
477 3. Lin W, Jiang W, Hu X, Gao L, Ai D, Pan H, et al. Ecological Shifts of
478 Supragingival Microbiota in Association with Pregnancy. Frontiers in Cellular and
479 Infection Microbiology. 2018;8.
480 4. Paropkari AD, Leblebicioglu B, Christian LM, Kumar PS. Smoking, pregnancy
481 and the subgingival microbiome. Sci Rep. 2016;6(1):30388.

482 5. Jang H, Patoine A, Wu TT, Castillo DA, Xiao J. Oral microflora and pregnancy: a
483 systematic review and meta-analysis. Sci Rep. 2021;11(1):16870.
484 6. Powell AM, Khan FZA, Ravel J, Elovitz MA. Untangling Associations of
485 Microbiomes of Pregnancy and Preterm Birth. Clinics in Perinatology. 2024;51(2):425-
486 39.
487 7. Wen P, Li H, Xu X, Zhang F, Zhao D, Yu R, et al. A prospective study on
488 maternal periodontal diseases and neonatal adverse outcomes. Acta Odontol Scand.
489 2024;83:348-55.
490 8. Kassebaum NJ, Bernabé E, Dahiya M, Bhandari B, Murray CJL, Marcenes W.
491 Global Burden of Severe Periodontitis in 1990-2010:A Systematic Review and Meta-
492 regression. Journal of Dental Research. 2014;93(11):1045-53.
493 9. Lieff S, Boggess KA, Murtha AP, Jared H, Madianos PN, Moss K, et al. The Oral
494 Conditions and Pregnancy Study: Periodontal Status of a Cohort of Pregnant Women.
495 Journal of Periodontology. 2004;75(1):116-26.
496 10. Kornman KS, Loesche WJ. The subgingival microbial flora during pregnancy. J
497 Periodontal Res. 1980;15(2):111-22.
498 11. Reyes L, Phillips P, Wolfe B, Golos TG, Walkenhorst M, Progulske-Fox A, et al.
499 Porphyromonas gingivalis and adverse pregnancy outcome. J Oral Microbiol.
500 2018;10(1):1374153.
501 12. Silva de Araujo Figueiredo C, Gonçalves Carvalho Rosalem C, Costa
502 Cantanhede AL, Abreu Fonseca Thomaz ÉB, Fontoura Nogueira da Cruz MC. Systemic
503 alterations and their oral manifestations in pregnant women. Journal of Obstetrics and
504 Gynaecology Research. 2017;43(1):16-22.

505 13. Chaparro A, Blanlot C, Ramirez V, Sanz A, Quintero A, Inostroza C, et al.
506 Porphyromonas gingivalis, Treponema denticola and toll-like receptor 2 are associated
507 with hypertensive disorders in placental tissue: a case-control study. J Periodontal Res.
508 2013;48(6):802-9.
509 14. Ercan E, Eratalay K, Deren O, Gur D, Ozyuncu O, Altun B, et al. Evaluation of
510 periodontal pathogens in amniotic fluid and the role of periodontal disease in pre-term
511 birth and low birth weight. Acta Odontol Scand. 2013;71(3-4):553-9.
512 15. Gonzales-Marin C, Spratt DA, Millar MR, Simmonds M, Kempley ST, Allaker RP.
513 Levels of periodontal pathogens in neonatal gastric aspirates and possible maternal
514 sites of origin. Mol Oral Microbiol. 2011;26(5):277-90.
515 16. Katz J, Chegini N, Shiverick KT, Lamont RJ. Localization of P. gingivalis in
516 preterm delivery placenta. J Dent Res. 2009;88(6):575-8.
517 17. Leon R, Silva N, Ovalle A, Chaparro A, Ahumada A, Gajardo M, et al. Detection
518 of Porphyromonas gingivalis in the amniotic fluid in pregnant women with a diagnosis of
519 threatened premature labor. J Periodontol. 2007;78(7):1249-55.
520 18. Swati P, Ambika Devi K, Thomas B, Vahab SA, Kapaettu S, Kushtagi P.
521 Simultaneous detection of periodontal pathogens in subgingival plaque and placenta of
522 women with hypertension in pregnancy. Arch Gynecol Obstet. 2012;285(3):613-9.
523 19. Ishida E, Furusho H, Renn T-Y, Shiba F, Chang H-M, Oue H, et al. Mouse
524 maternal odontogenic infection with Porphyromonas gingivalis induces cognitive decline
525 in offspring. Frontiers in Pediatrics. 2023;11.
526 20. Lara B, Loureiro I, Gliosca L, Castagnola L, Merech F, Gallino L, et al.
527 Porphyromonas gingivalis outer membrane vesicles shape trophoblast cell metabolism

528 impairing functions associated to adverse pregnancy outcome. Journal of Cellular
529 Physiology. 2023;238(11):2679-91.
530 21. Ao M, Miyauchi M, Furusho H, Inubushi T, Kitagawa M, Nagasaki A, et al. Dental
531 Infection of Porphyromonas gingivalis Induces Preterm Birth in Mice. PLOS ONE.
532 2015;10(8):e0137249.
533 22. Konishi H, Urabe S, Miyoshi H, Teraoka Y, Maki T, Furusho H, et al. Fetal
534 Membrane Inflammation Induces Preterm Birth Via Toll-Like Receptor 2 in Mice With
535 Chronic Gingivitis. Reprod Sci. 2019;26(7):869-78.
536 23. Konishi H, Urabe S, Teraoka Y, Morishita Y, Koh I, Sugimoto J, et al.
537 Porphyromonas gingivalis, a cause of preterm birth in mice, induces an inflammatory
538 response in human amnion mesenchymal cells but not epithelial cells. Placenta.
539 2020;99:21-6.
540 24. Lin D, Smith MA, Champagne C, Elter J, Beck J, Offenbacher S. Porphyromonas
541 gingivalis infection during pregnancy increases maternal tumor necrosis factor alpha,
542 suppresses maternal interleukin-10, and enhances fetal growth restriction and
543 resorption in mice. Infect Immun. 2003;71(9):5156-62.
544 25. Yoshida S, Hatasa M, Ohsugi Y, Tsuchiya Y, Liu A, Niimi H, et al.
545 Porphyromonas gingivalis Administration Induces Gestational Obesity, Alters Gene
546 Expression in the Liver and Brown Adipose Tissue in Pregnant Mice, and Causes
547 Underweight in Fetuses. Frontiers in Cellular and Infection Microbiology. 2022;11.
548 26. Choi J-W, Kim S-C, Hong S-H, Lee H-J. Secretable Small RNAs via Outer
549 Membrane Vesicles in Periodontal Pathogens. Journal of Dental Research.
550 2017;96(4):458-66.

551 27. Gui MJ, Dashper SG, Slakeski N, Chen Y-Y, Reynolds EC. Spheres of influence:
552 Porphyromonas gingivalis outer membrane vesicles. Molecular Oral Microbiology.
553 2016;31(5):365-78.
554 28. Ho M-H, Chen C-H, Goodwin JS, Wang B-Y, Xie H. Functional Advantages of
555 Porphyromonas gingivalis Vesicles. PLOS ONE. 2015;10(4):e0123448.
556 29. Okamura H, Hirota K, Yoshida K, Weng Y, He Y, Shiotsu N, et al. Outer
557 membrane vesicles of Porphyromonas gingivalis: Novel communication tool and
558 strategy. Japanese Dental Science Review. 2021;57:138-46.
559 30. Veith PD, Chen Y-Y, Gorasia DG, Chen D, Glew MD, O'Brien-Simpson NM, et al.
560 Porphyromonas gingivalis Outer Membrane Vesicles Exclusively Contain Outer
561 Membrane and Periplasmic Proteins and Carry a Cargo Enriched with Virulence
562 Factors. Journal of Proteome Research. 2014;13(5):2420-32.
563 31. Zhang J, Yu C, Zhang X, Chen H, Dong J, Lu W, et al. Porphyromonas gingivalis
564 lipopolysaccharide induces cognitive dysfunction, mediated by neuronal inflammation
565 via activation of the TLR4 signaling pathway in C57BL/6 mice. J Neuroinflammation.
566 2018;15(1):37.
567 32. Nara PL, Sindelar D, Penn MS, Potempa J, Griffin WST. Porphyromonas
568 gingivalis Outer Membrane Vesicles as the Major Driver of and Explanation for
569 Neuropathogenesis, the Cholinergic Hypothesis, Iron Dyshomeostasis, and Salivary
570 Lactoferrin in Alzheimer's Disease. J Alzheimers Dis. 2021;82(4):1417-50.
571 33. Gong T, Chen Q, Mao H, Zhang Y, Ren H, Xu M, et al. Outer membrane vesicles
572 of Porphyromonas gingivalis trigger NLRP3 inflammasome and induce

573 neuroinflammation, tau phosphorylation, and memory dysfunction in mice. Front Cell
574 Infect Microbiol. 2022;12:925435.
575 34. Lan C, Chen S, Jiang S, Lei H, Cai Z, Huang X. Different expression patterns of
576 inflammatory cytokines induced by lipopolysaccharides from Escherichia coli or
577 Porphyromonas gingivalis in human dental pulp stem cells. BMC Oral Health.
578 2022;22(1):121.
579 35. Qiu C, Yuan Z, He Z, Chen H, Liao Y, Li S, et al. Lipopolysaccharide Preparation
580 Derived From Porphyromonas gingivalis Induces a Weaker Immuno-Inflammatory
581 Response in BV-2 Microglial Cells Than Escherichia coli by Differentially Activating
582 TLR2/4-Mediated NF-κB/STAT3 Signaling Pathways. Frontiers in Cellular and Infection
583 Microbiology. 2021;11.
584 36. Bodet C, Chandad F, Grenier D. Modulation of cytokine production by
585 Porphyromonas gingivalis in a macrophage and epithelial cell co-culture model.
586 Microbes and Infection. 2005;7(3):448-56.
587 37. Castillo Y, Castellanos JE, Lafaurie GI, Castillo DM. Porphyromonas gingivalis
588 outer membrane vesicles modulate cytokine and chemokine production by gingipain-
589 dependent mechanisms in human macrophages. Archives of Oral Biology.
590 2022;140:105453.
591 38. Charoensaensuk V, Chen YC, Lin YH, Ou KL, Yang LY, Lu DY. Porphyromonas
592 gingivalis Induces Proinflammatory Cytokine Expression Leading to Apoptotic Death
593 through the Oxidative Stress/NF-κB Pathway in Brain Endothelial Cells. Cells.
594 2021;10(11).

595 39. Palm E, Khalaf H, Bengtsson T. Porphyromonas gingivalis downregulates the
596 immune response of fibroblasts. BMC Microbiology. 2013;13(1):155.
597 40. Yang K, Xu S, Zhao H, Liu L, Lv X, Hu F, et al. Hypoxia and Porphyromonas
598 gingivalis-lipopolysaccharide synergistically induce NLRP3 inflammasome activation in
599 human gingival fibroblasts. International Immunopharmacology. 2021;94:107456.
600 41. Offenbacher S, Katz V, Fertik G, Collins J, Boyd D, Maynor G, et al. Periodontal
601 infection as a possible risk factor for preterm low birth weight. J Periodontol. 1996;67(10
602 Suppl):1103-13.
603 42. Zhang B, Wei YZ, Wang GQ, Li DD, Shi JS, Zhang F. Targeting MAPK Pathways
604 by Naringenin Modulates Microglia M1/M2 Polarization in Lipopolysaccharide-
605 Stimulated Cultures. Front Cell Neurosci. 2018;12:531.
606 43. Frank-Cannon TC, Alto LT, McAlpine FE, Tansey MG. Does neuroinflammation
607 fan the flame in neurodegenerative diseases? Mol Neurodegener. 2009;4:47.
608 44. Gao Y, Tan L, Yu JT, Tan L. Tau in Alzheimer's Disease: Mechanisms and
609 Therapeutic Strategies. Curr Alzheimer Res. 2018;15(3):283-300.
610 45. Morris SL, Brady ST. Tau phosphorylation and PAD exposure in regulation of
611 axonal growth. Frontiers in Cell and Developmental Biology. 2023;10.
612 46. Seubert P, Mawal-Dewan M, Barbour R, Jakes R, Goedert M, Johnson GV, et al.
613 Detection of phosphorylated Ser262 in fetal tau, adult tau, and paired helical filament
614 tau. J Biol Chem. 1995;270(32):18917-22.
615 47. Brion J-P, Smith C, Couck A-M, Gallo J-M, Anderton BH. Developmental
616 Changes in τ Phosphorylation: Fetal τ Is Transiently Phosphorylated in a Manner Similar

617 to Paired Helical Filament-τ Characteristic of Alzheimer's Disease. Journal of
618 Neurochemistry. 1993;61(6):2071-80.
619 48. Tang Z, Liang D, Cheng M, Su X, Liu R, Zhang Y, et al. Effects of
620 Porphyromonas gingivalis and Its Underlying Mechanisms on Alzheimer-Like Tau
621 Hyperphosphorylation in Sprague-Dawley Rats. Journal of Molecular Neuroscience.
622 2021;71(1):89-100.
623 49. Yu Y, Run X, Liang Z, Li Y, Liu F, Liu Y, et al. Developmental regulation of tau
624 phosphorylation, tau kinases, and tau phosphatases. J Neurochem. 2009;108(6):1480-
625 94.
626 50. Arendt T, Stieler JT, Holzer M. Tau and tauopathies. Brain Res Bull. 2016;126(Pt
627 3):238-92.
628 51. Wang C, Fan L, Khawaja RR, Liu B, Zhan L, Kodama L, et al. Microglial NF-κB
629 drives tau spreading and toxicity in a mouse model of tauopathy. Nature
630 Communications 2015 6. 2022;13(1):1969.
631 52. Perea JR, Ávila J, Bolós M. Dephosphorylated rather than hyperphosphorylated
632 Tau triggers a pro-inflammatory profile in microglia through the p38 MAPK pathway.
633 Experimental Neurology. 2018;310:14-21.
634 53. Hefti MM, Kim S, Bell AJ, Betters RK, Fiock KL, Iida MA, et al. Tau
635 Phosphorylation and Aggregation in the Developing Human Brain. J Neuropathol Exp
636 Neurol. 2019;78(10):930-8.
637 54. Sapir T, Frotscher M, Levy T, Mandelkow EM, Reiner O. Tau's role in the
638 developing brain: implications for intellectual disability. Hum Mol Genet.
639 2012;21(8):1681-92.

640 55. Mishra A, Bandopadhyay R, Singh PK, Mishra PS, Sharma N, Khurana N.
641 Neuroinflammation in neurological disorders: pharmacotherapeutic targets from bench
642 to bedside. Metab Brain Dis. 2021;36(7):1591-626.
643 56. Mashburn LM, Whiteley M. Membrane vesicles traffic signals and facilitate group
644 activities in a prokaryote. Nature. 2005;437(7057):422-5.
645 57. Lambert J-F, Benoit BO, Colvin GA, Carlson J, Delville Y, Quesenberry PJ. Quick
646 sex determination of mouse fetuses. Journal of Neuroscience Methods. 2000;95(2):127-
647 32.
648

649 # Supporting Information

650

651 S1. Iba-1 and Thr231 western blots.

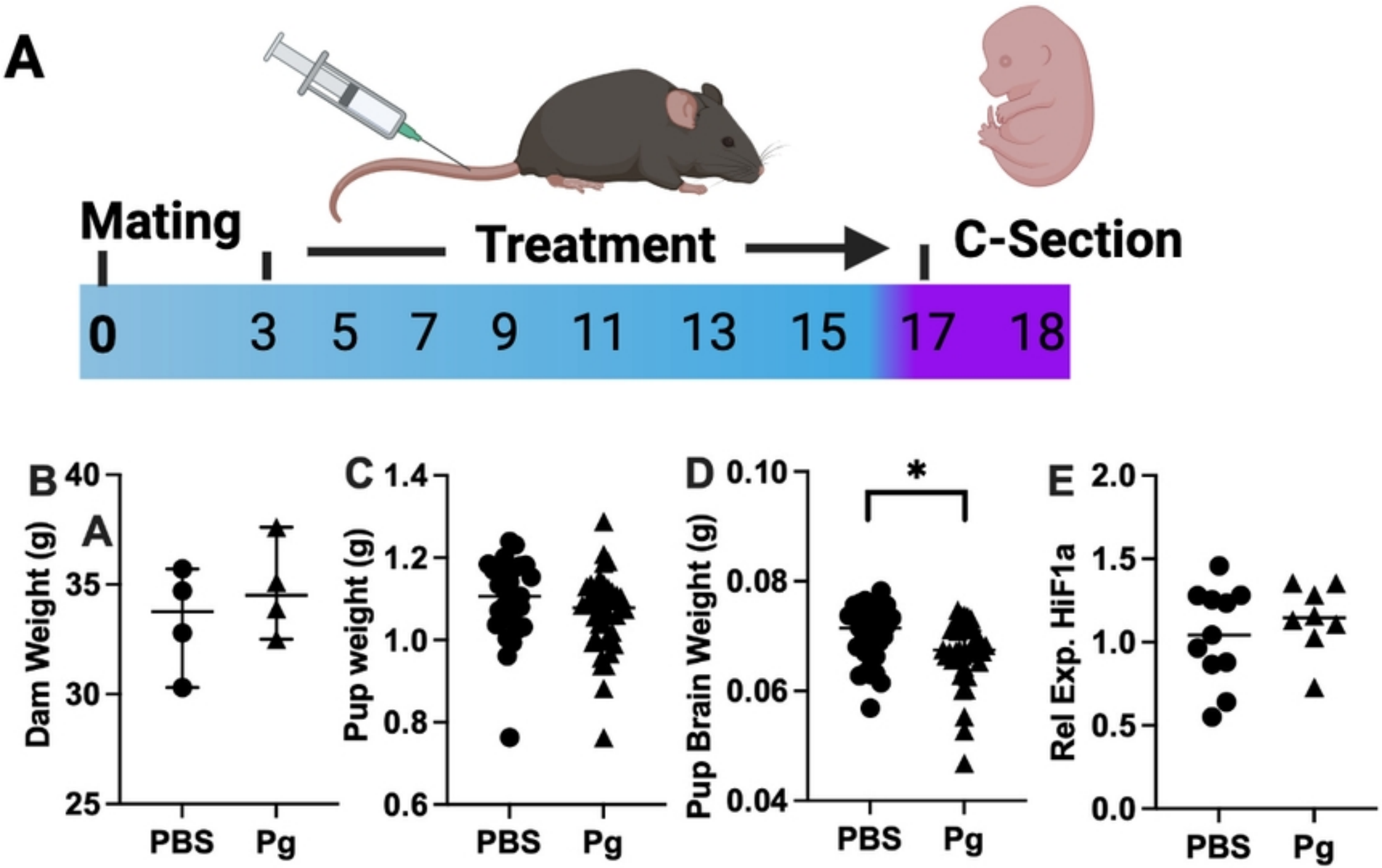
A
Mating
Treatment
C-Section
0
3
5
7
9
11
13
15
17
18
B
A
Dam Weight (g)
40
35
30
25
PBS
Pg
C
Pup weight (g)
1.4
1.2
1.0
0.8
0.6
PBS
Pg
D
Pup Brain Weight (g)
0.10
0.08
0.06
0.04
*
PBS
Pg
E
Rel Exp. HiF1a
2.0
1.5
1.0
0.5
0.0
PBS
Pg

Fig 1

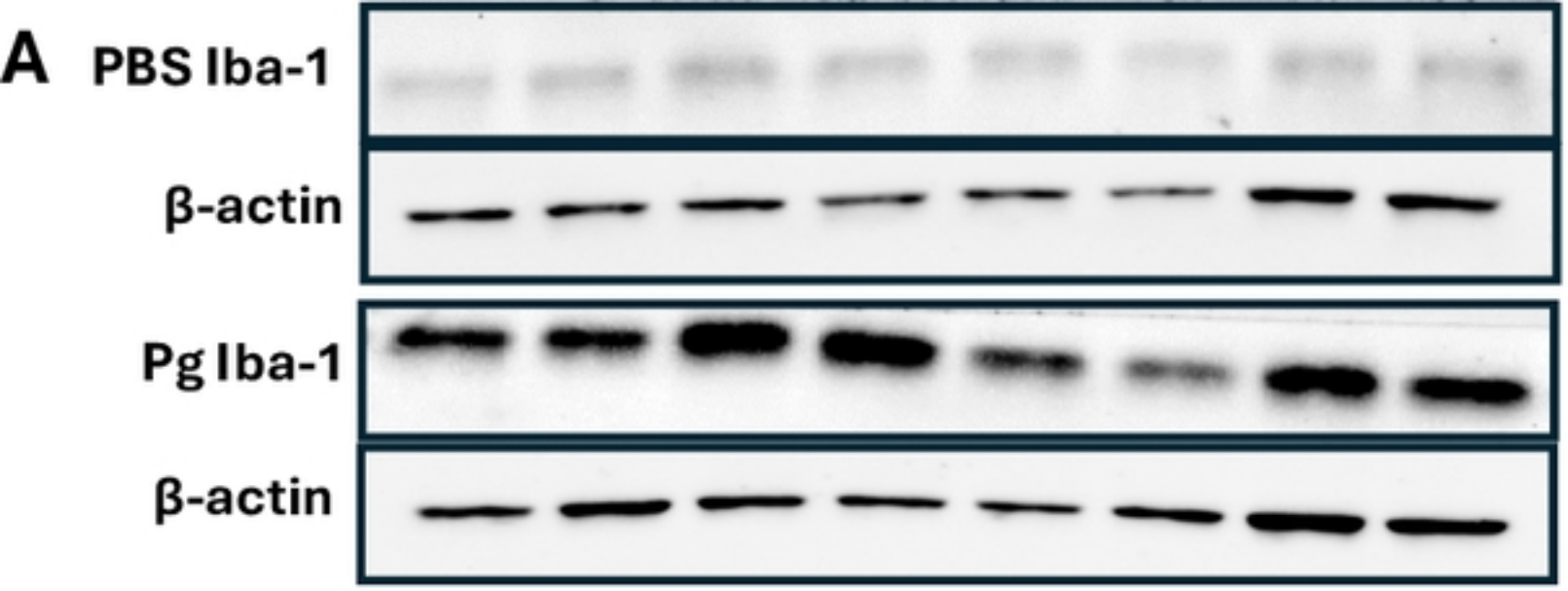
A
PBS Iba-1
β-actin
Pg Iba-1
β-actin

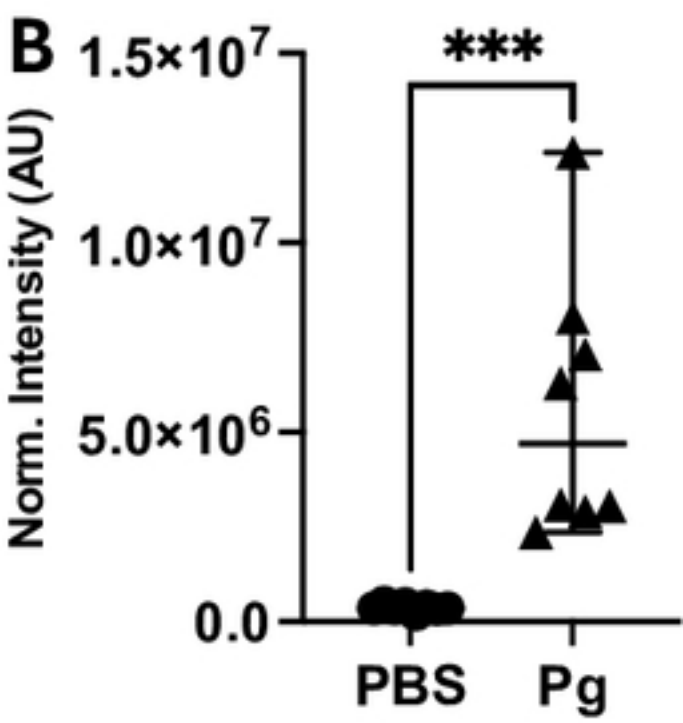
B
1.5×10^7
1.0×10^7
5.0×10^6
0.0
Norm. Intensity (AU)
***
PBS
Pg

Manuscript

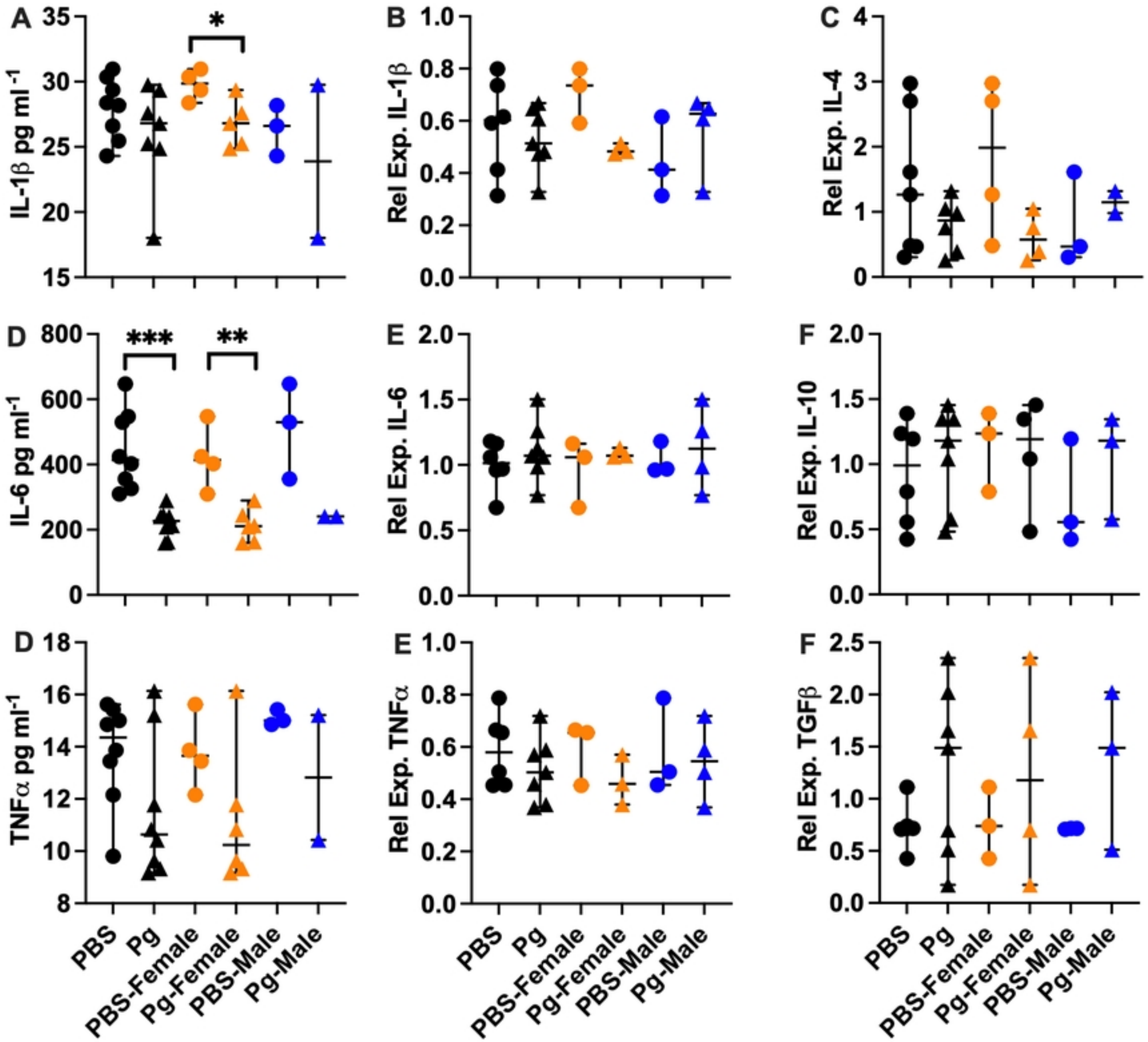
A
IL-1β pg ml-1
35
30
25
20
15
*
B
Rel Exp. IL-1β
1.0
0.8
0.6
0.4
0.2
0.0
C
Rel Exp. IL-4
4
3
2
1
0
D
IL-6 pg ml-1
800
600
400
200
0
***
**
E
Rel Exp. IL-6
2.0
1.5
1.0
0.5
0.0
F
Rel Exp. IL-10
2.0
1.5
1.0
0.5
0.0
D
TNFα pg ml-1
18
16
14
12
10
8
E
Rel Exp. TNFα
1.0
0.8
0.6
0.4
0.2
0.0
F
Rel Exp. TGFβ
2.5
2.0
1.5
1.0
0.5
0.0
PBS
Pg
PBS-Female
Pg-Female
PBS-Male
Pg-Male

Fig 3

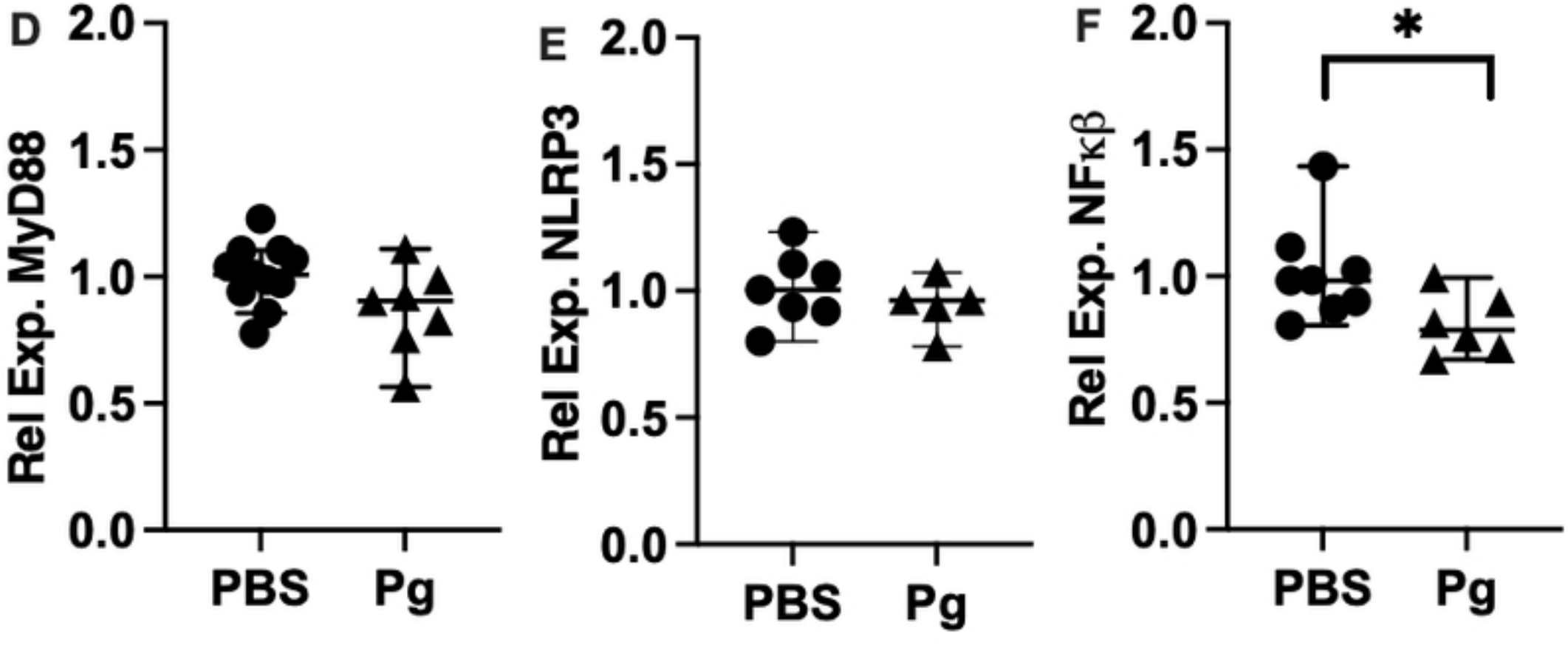
D
Rel Exp. MyD88
2.0
1.5
1.0
0.5
0.0
PBS
Pg
E
Rel Exp. NLRP3
2.0
1.5
1.0
0.5
0.0
PBS
Pg
F
Rel Exp. NFκβ
*
2.0
1.5
1.0
0.5
0.0
PBS
Pg

Fig 4

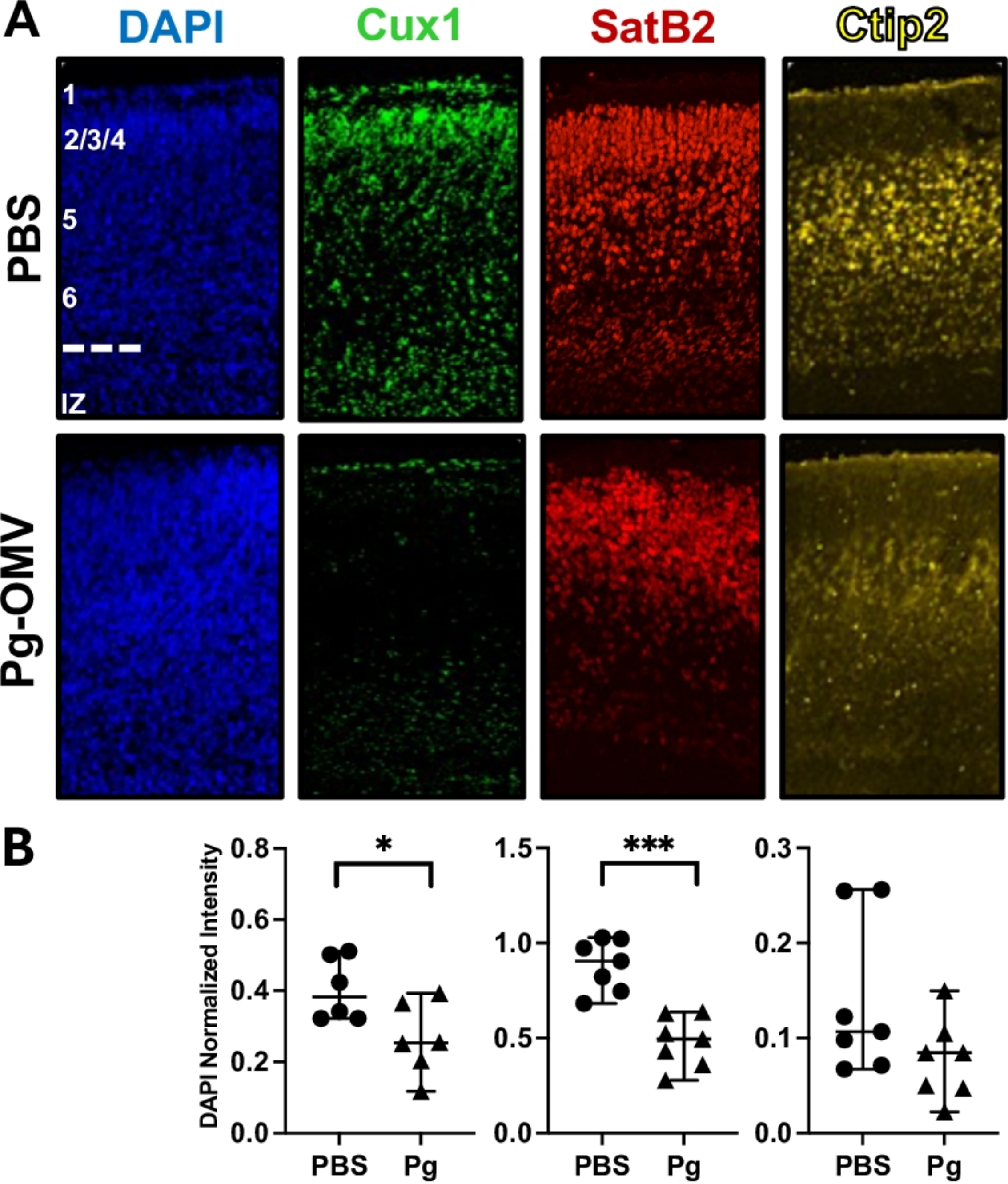
A
DAPI
Cux1
SatB2
Ctip2
PBS
Pg-OMV
1
2/3/4
5
6
IZ
B
DAPI Normalized Intensity
0.8
0.6
0.4
0.2
0.0
*
PBS
Pg
1.5
1.0
0.5
0.0
***
PBS
Pg
0.3
0.2
0.1
0.0
PBS
Pg

Fig 5

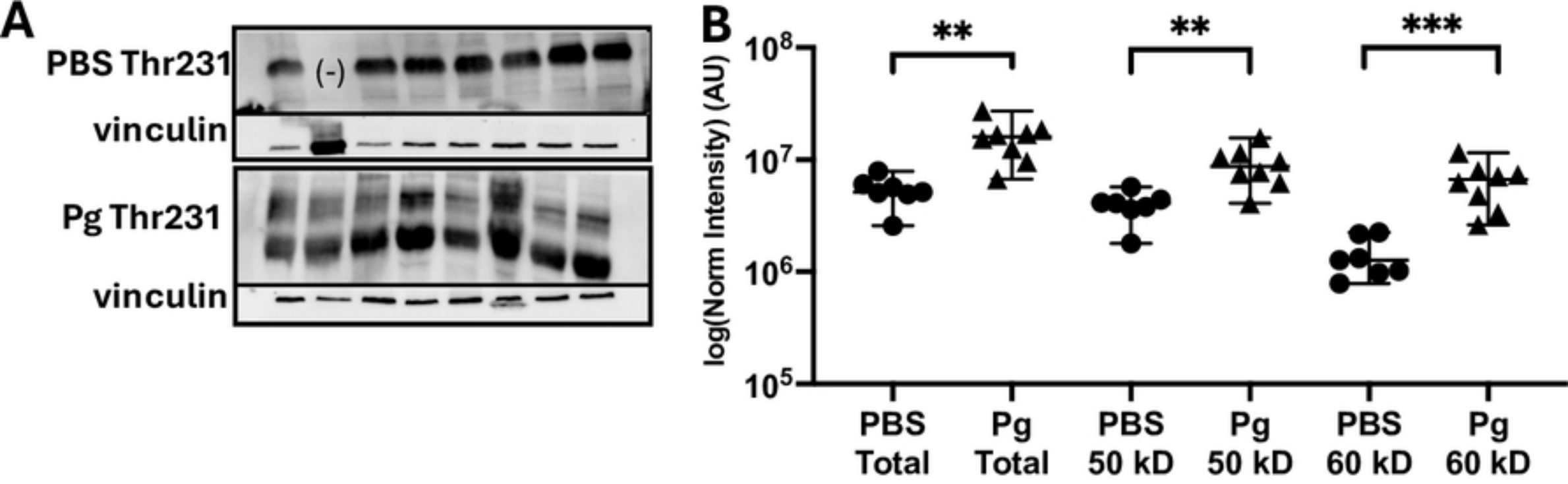
A
PBS Thr231
(-)
vinculin
Pg Thr231
vinculin
B
log(Norm Intensity) (AU)
10^8
10^7
10^6
10^5
**
**
***
PBS Total
Pg Total
PBS 50 kD
Pg 50 kD
PBS 60 kD
Pg 60 kD

Fig 6